

# Quantum Gates and Memory using Microwave Dressed States

N. Timoney, I. Baumgart, M. Johanning, A. F. Varón, and Ch. Wunderlich

*Department Physik, Naturwissenschaftlich-Technische Fakultät, Universität Siegen, 57068 Siegen, Germany*

M. B. Plenio and A. Retzker

*Institut für Theoretische Physik, Universität Ulm, 89069 Ulm, Germany*

(Dated: October 24, 2018)

Trapped atomic ions have been successfully used for demonstrating basic elements of universal quantum information processing (QIP) [1]. Nevertheless, scaling up of these methods and techniques to achieve large scale universal QIP, or more specialized quantum simulations [2–5] remains challenging. The use of easily controllable and stable microwave sources instead of complex laser systems [6, 7] on the other hand promises to remove obstacles to scalability. Important remaining drawbacks in this approach are the use of magnetic field sensitive states, which shorten coherence times considerably, and the requirement to create large stable magnetic field gradients. Here, we present theoretically a novel approach based on dressing magnetic field sensitive states with microwave fields which addresses both issues and permits fast quantum logic. We experimentally demonstrate basic building blocks of this scheme to show that these dressed states are long-lived and coherence times are increased by more than two orders of magnitude compared to bare magnetic field sensitive states. This changes decisively the prospect of microwave-driven ion trap QIP and offers a new route to extend coherence times for all systems that suffer from magnetic noise such as neutral atoms, NV-centres, quantum dots, or circuit-QED systems.

*Introduction* — Using laser light for coherent manipulation of qubits gives rise to fundamental issues, notably, unavoidable spontaneous emission which destroys quantum coherence [8, 9]. The difficulty in cooling a collection of ions to their motional ground state and the time needed for such a process in the presence of spurious heating of Coulomb crystals limits the fidelity of quantum logic operations in laser-based quantum gates, and thus hampers scalability. This limitation is only partially removed by the use of ‘hot’ gates [10, 11]. Technical challenges in accurately controlling the frequency and intensity of laser light as well as delivering a large number of laser beams of high intensity to trapped ions are further obstacles for scalability.

These issues associated with the use of laser light for scalable QIP have led to the development of novel concepts for performing conditional quantum dynamics with trapped ions that rely on radio frequency (rf) or microwave (mw) radiation instead of laser light [6, 7, 12–15]. Rf or mw radiation can be employed for quantum gates through the use of magnetic gradient induced coupling (MAGIC) between spin states of ions [16], thus averting technical and fundamental issues of scalability that were described above. Furthermore, the sensitivity to motional excitation of ions is reduced in such schemes. A drawback of MAGIC is the necessity to use magnetic field sensitive states for conditional quantum dynamics, thus making qubits susceptible to ambient field noise and shortening their coherence time. This issue is shared with some optical ion trap schemes for QIP that usually rely on magnetic field sensitive states for conditional quantum dynamics, like geometric gates [1], limiting the coherence time of qubit states typically to a few ms. In an effort to extend the coherence time of atomic states, two-qubit entangled states forming a decoherence-free subspace have been created [17, 18]. Recently, transfer between field sensitive states, that are used for conditional quantum dynamics and field insensitive states used for storage of quantum information has been employed [19].

The relevant noise source in this case, namely magnetic field fluctuations, is not featureless white noise but tends to have a limited bandwidth. In this context techniques were proposed for prolonging coherence times by subjecting the system to a rapid succession of pulses leading to a decoupling from the environment. This technique, termed Bang Bang control [20], and its continuous version [21] can be applied to advantage in a variety of systems including hybrid atomic and nano-physics technologies. Recent work includes the experimental demonstration of optimized pulse sequences made for suppression of qubit decoherence ([22, 23] and references therein).

Here, we encode qubits in microwave dressed states requiring only continuous, constant intensity microwave fields. This scheme protects qubits from magnetic field fluctuations and, importantly, allows at the same time to perform fast quantum gates even for small Lamb-Dicke parameters, and therefore moderate magnetic field gradients. Microwave generating elements for coherent manipulation of qubits can be integrated in micro-structured ion traps [7] such that quantum information processing can be realized using scalable ion chips. Thus, this novel scheme is a significant step on the route towards integrating elements required for quantum information processing on a scalable ion chip. Moreover, the ideas presented here are generic and can be applied to all laser- or microwave-based QIP such as neutral atoms, NV-centres and quantum dots.

We describe theoretically the scheme for storage, single and multi-qubit quantum gate operation and then present experimental demonstrations of storage and information processing of quantum information that demonstrate gains of two orders of magnitude in coherence times.

*Theory of dressed state memory and single-qubit* — We consider a typical energy level configuration depicted in Fig. 1a. Encoding quantum information in the subspace spanned by two magnetically sensitive  $m_F = \pm 1$  states ( $|-1\rangle, | +1\rangle$ ) will lead to a rapid loss of coherence due to fluctuating magnetic fields. We first note that microwave-dressed states (with Rabi frequency  $\Omega$  and detunings  $\Delta_-$  and  $\Delta_+$  which are optimally equal) create a subspace spanned by the two states  $|D\rangle = (|-1\rangle - |+1\rangle)/\sqrt{2}$  and  $|0'\rangle$  ( $m_F = 0$ ) of the same manifold that is separated from the other eigenstates  $|u\rangle$  and  $|d\rangle$  of the system by a finite energy gap. The energetically degenerate states  $|D\rangle$  and  $|0'\rangle$  are not coupled by magnetic field fluctuations. As a consequence of the energy gap to the states  $|u\rangle$  and  $|d\rangle$ , a relative phase change between states  $|-1\rangle$  and  $|+1\rangle$  now acquires an energy penalty and dephasing is strongly suppressed as long as the spectral power density of the magnetic field fluctuations at the frequency corresponding to the energy gap is negligible. Note however that the levels  $|D\rangle$  and  $|0'\rangle$  are energetically degenerate independent of the applied microwave Rabi-frequency  $\Omega$  and hence stable against its fluctuations. Hence we will consider the qubit encoded in the subspace spanned by  $|D\rangle$  and  $|0'\rangle$ . In this case, the dephasing time would be limited by second order effects in the magnetic field fluctuations which in our case leads to a lifetime of the order 1 s. The nature of the protected subspace depends on the relative phase between the microwave fields on the transitions  $|0\rangle \leftrightarrow |\pm 1\rangle$ . The above description applies for a relative phase 0 while for a relative phase of  $\pi$ , the protected subspace is spanned by  $|B\rangle = (|-1\rangle + |+1\rangle)/\sqrt{2}$  and  $|0'\rangle$ . We have implemented both settings in the experiments reported below.

The application of additional rf fields (with Rabi frequency  $\Omega_g$  and possible detuning  $\Delta_g$ ) and relative phase  $\pi$  then permits the implementation of general single qubit rotations in the protected subspace spanned by  $|D\rangle$  and  $|0'\rangle$ . Choosing  $\Delta_g = 0$  yields the Hamiltonian  $H = \Omega_g (|D\rangle\langle 0'| + |0'\rangle\langle D|)$  which describes arbitrary rotations about the

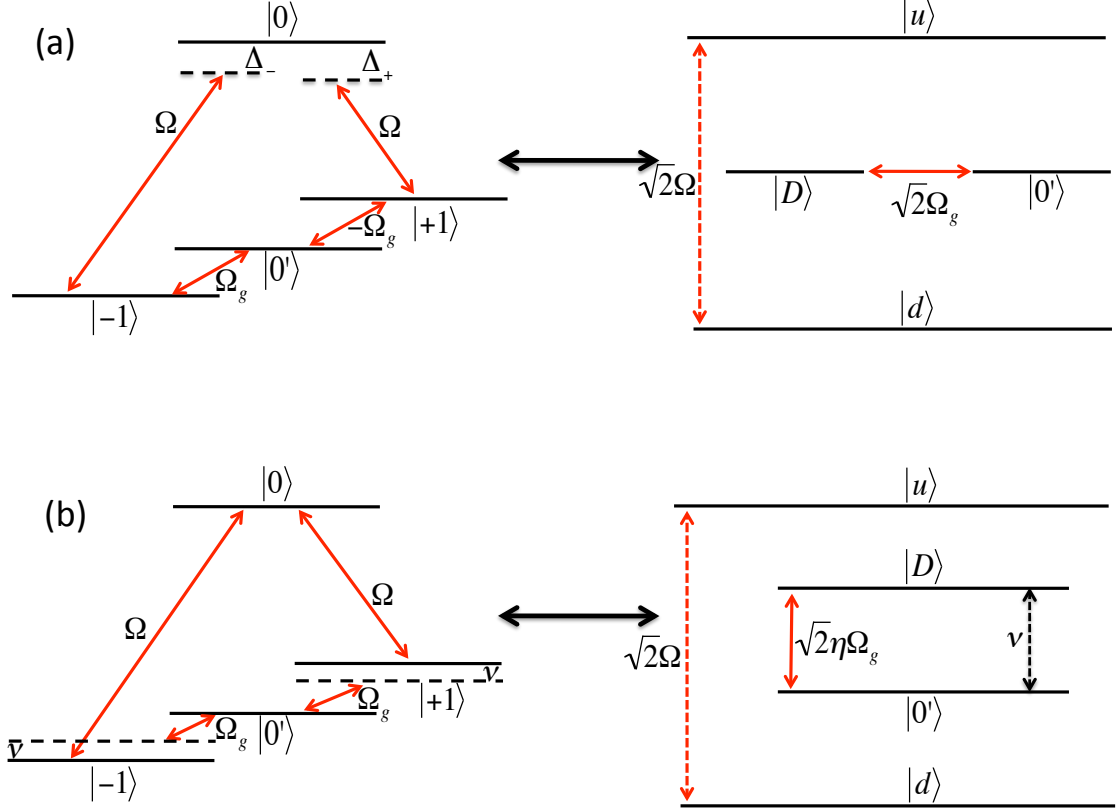


FIG. 1. Microwave-dressed qubit states.  $|-1\rangle$  and  $|+1\rangle$  represent internal magnetic sensitive states, e.g.  $m_F = \pm 1$ , and  $|0\rangle$  and  $|0'\rangle$  represent two additional magnetically insensitive levels (e.g.  $m_F = 0$  states of two different hyperfine manifolds). The application of microwave radiation, with Rabi frequency  $\Omega$ , induces a dressed-state basis where the states  $|D\rangle = (|-1\rangle - |+1\rangle)/\sqrt{2}$  and  $|0'\rangle$  are separated by an energy gap from the other two states,  $|u\rangle = (|B\rangle + |0\rangle)/\sqrt{2}$  and  $|d\rangle = (|B\rangle - |0\rangle)/\sqrt{2}$ , where  $|B\rangle = (|-1\rangle + |+1\rangle)/\sqrt{2}$ . This arrangement creates a qubit in  $|D\rangle$  and  $|0'\rangle$  that is resilient to magnetic field fluctuations – since phase changes are now suppressed by an energy gap – and to microwave power fluctuations, since the energy gap between  $|D\rangle$  and  $|0'\rangle$  does not depend on microwave power. As shown in part (a), an rf field with Rabi frequency  $\Omega_g$  and detuning  $\Delta_g$ , which should be equal to  $\nu$  for a multi-qubit gate and should be zero for a single-qubit gate, can be used to implement general single qubit quantum gates. The right part is the the frame which rotates with the driving frequencies (dressed states). Conditional quantum dynamics coupling electronic degrees of freedom to the motion can be achieved (see (b)) in the presence of a magnetic field gradient when an rf field that is detuned from the carrier transition of the qubit by the vibrational frequency  $\nu$ . In this case the  $|D\rangle$  and  $|0'\rangle$  are not degenerate but have an energy gap which is the rf detuning. The atomic hyperfine states of  $^{171}\text{Yb}^+$  used in this work can be mapped to the general scheme shown here as follows:  $|F = 0\rangle \leftrightarrow |0\rangle$ ,  $|F = 1, m_F = -1\rangle \leftrightarrow |-1\rangle$ ,  $|F = 1, m_F = +1\rangle \leftrightarrow |+1\rangle$ ,  $|F = 1, m_F = 0\rangle \leftrightarrow |0'\rangle$

$x$  - axis in the protected space. A rotation about the z-axis is obtained for  $\Omega_g, \nu \ll \Delta_g \neq 0$ . The specific case  $\Delta_g = \nu$ , i.e. tuning to the motional sideband will be discussed later as it couples the electronic to the motional degree of freedom.

*Experimental realization* – Hyperfine states of electrodynamically trapped  $^{171}\text{Yb}^+$  ions characterized by quantum numbers  $F = 0$  and  $F = 1$  in the electronic ground state  $S_{1/2}$  are used in the experiments reported here (see the caption of Fig. 1). State-selective detection is achieved by collecting scattered fluorescence on the  $(S_{1/2}, F = 1) - (P_{1/2}, F = 0)$  resonance which allows for discriminating population in states  $S_{1/2}, F = 0$  (no fluorescence) and  $S_{1/2}, F = 1$  (resonance fluorescence is detected).

The procedure to generate and detect dressed states can be thought of as being divided into three segments (compare inset of Fig. 2): First (up to time  $t = T_1$ ), an incomplete stimulated rapid adiabatic passage (STIRAP) [24] is used to adiabatically transfer the system from the atomic to the dressed state basis. Second (up to  $t = T_2$ ), the amplitudes of the dressing fields are kept constant for a holding time  $T = T_2 - T_1$ , since we are interested in creating and utilising dressed states (as opposed to population transfer). Between  $t = T_1$  and  $t = T_2$  dressed states are present (right-hand-side of Figs.1a and 1b) and quantum operations with them are implemented, for example, through application

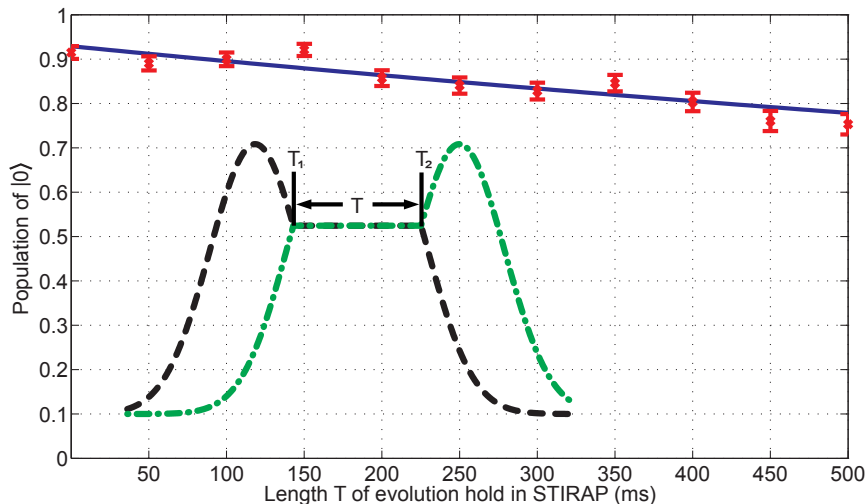


FIG. 2. Lifetime of the dressed state  $|D\rangle$ . The inset shows the qualitative temporal behaviour of the two dressing fields' amplitudes. In order to prepare the dressed state  $|D\rangle$ , the dressing field's amplitudes are ramped up adiabatically until time  $T_1$ . Then, the amplitudes of these dressing fields are kept constant until time  $T_2$ , the STIRAP sequence is completed adiabatically transferring the dressed state  $|D\rangle$  back to a bare ionic state. The hold time  $T = T_2 - T_1$ . The solid line represents a fitted exponential giving a lifetime of  $1700 \pm 300$  ms. Both microwave dressing fields are set on resonance with the atomic transitions (in the bare state picture they drive the  $|-1\rangle - |0\rangle$  and the  $|+1\rangle - |0\rangle$  transitions). The adiabatic (STIRAP) preparation is characterized by these parameters: pulse separation of  $6/f_\Omega$ , pulse width of  $5/f_\Omega$  and  $\Delta t = \frac{1}{10f_\Omega}$ , where  $f_\Omega = \Omega/(2\pi) = 36.5$  kHz. The microwave frequency on the  $|+1\rangle - |0\rangle$  resonance was 12.6528121 GHz, and on the on the  $|-1\rangle - |0\rangle$  resonance it was 12.6328272 GHz; a static magnetic field  $B = 0.714$  mT defines a quantization axis. Each measurement point consists of 300 repetitions.

of additional rf fields. For a single-qubit gate between dressed states (Fig. 1a rhs), the rf field is on resonance with the  $|0'\rangle \leftrightarrow |+1\rangle, |-1\rangle$  transition, and for a multi-qubit gate (Fig. 1b) the rf is detuned by the vibrational mode frequency  $\nu$  from this transition. Third ( $t > T_2$ ), the STIRAP sequence is completed when the ion is transferred from the dressed state basis back to the atomic states. Any dephasing of a dressed state or transitions to other states during the holding time  $T$  gives rise to imperfect population transfer during step three of this sequence that returns the system to the atomic state basis. This is described in more detail in the Methods section for the creation and detection of the  $|D\rangle$  state.

*Preparation and lifetime of state  $|D\rangle$*  – Fig. 2 presents the effectiveness of preparation and detection of state  $|D\rangle$  as a function of the holding time  $T$ . The measurement shown there extends over 500 ms and an exponential fit of the data yields a lifetime of this state of  $1700 \pm 300$  ms. This lifetime is limited by magnetic field fluctuations that couple the  $|D\rangle$  state to other states and the creation of a different dark state through phase fluctuations between the two microwave fields. This represents a remarkable improvement by more than two orders of magnitude in the dependance on the magnetic fluctuations, as the dephasing time of magnetically sensitive bare atomic states  $|\pm 1\rangle$  in this apparatus has a measured coherence time not exceeding 5.3 ms.

We have investigated the effectiveness of the STIRAP process for creating dressed states and transferring them into the final state as a function of the parameters characterizing the pulse sequence and found this technique to be robust over a wide range of experimental parameters (see Methods).

*Single qubit gates and coherence times of dressed state qubit* – As explained, our scheme permits the implementation of general single-qubit rotations in the subspace spanned by  $\{|0'\rangle, |D\rangle\}$  whose states are resilient not only to magnetic field fluctuations but also to variations in the amplitude of the dressing fields. The reason for this is that magnetic fluctuations couple the  $|B\rangle$  to the  $|D\rangle$  state and since the magnetic field noise power spectrum is very small at the microwave driving frequency their effect is substantially reduced. The new dephasing time will be governed by second order corrections which will scale with  $(\frac{\Delta B}{\Omega})^2$  with respect to the original dephasing rate, where  $\Delta B$  is the amplitude of the fluctuations. Moreover, the microwave does not couple any states in the qubit subspace and thus does not limit the phase coherence.

In order to demonstrate the enhanced coherence time of this qubit, we have conducted Rabi- and Ramsey-type

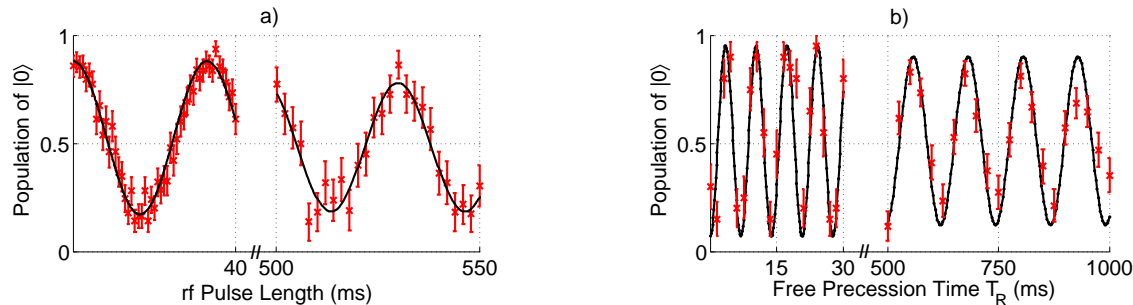


FIG. 3. Single-qubit gates with dressed states. a) Rabi oscillations between dressed state  $|B\rangle$  and  $|0'\rangle$  induced by an rf field for times up to more than 500 ms. Population in  $|B\rangle$  is mapped onto state  $|0\rangle$  at the end of the STIRAP and detection sequence (each datapoint is the average of 50 [up to 40 ms] or 25 repetitions [over 500 ms]). The microwave frequency on the  $|+1\rangle - |0\rangle$  resonance was 12.6533088 GHz, and on the  $|-1\rangle - |0\rangle$  resonance it was 12.6323327 GHz; the microwave Rabi frequency  $\Omega = 31.8 \times 2\pi$  kHz; the rf frequency driving transitions between dressed states was set to 10.49676 MHz; a static magnetic field  $B = 0.749$  mT defines a quantization axis. b) Ramsey-type measurement preparing a coherent superposition of  $|B\rangle$  and  $|0'\rangle$  and probing it after time  $T_R$ . Two rf  $\pi/2$ -pulses separated by time  $T_R$  of free evolution are applied to the qubit transition. The rf is slightly detuned from resonance (near 10.265 MHz corresponding to the  $|-1\rangle - |0\rangle$  and  $|+1\rangle - |0\rangle$  transitions) yielding Ramsey fringes with period  $1/(144.4Hz)$  between 0.1 ms and 30 ms. For the measurement between 500 ms and 1000 ms the period is  $1/(8.069Hz)$  (0 ms - 30 ms: 20 repetitions per datapoint; 500 ms - 1000 ms: 40 repetitions). Here,  $f_\Omega = \Omega/(2\pi) = 37.3$  kHz. The microwave frequency on the  $|+1\rangle - |0\rangle$  resonance was 12.6530938 GHz, and on the  $|-1\rangle - |0\rangle$  resonance it was 12.6325472 GHz; a static magnetic field  $B = 0.730$  mT defines a quantization axis.

measurements. First we move the system to the dressed state basis and then apply additional rf-fields with Rabi-frequency  $\Omega_g$  that induce Rabi oscillations between the dressed states  $|B\rangle$  and  $|0'\rangle$ . Using the  $|B\rangle$  state (not subject to spontaneous decay) has the advantage that no phase of  $\pi$  between the rf-fields is needed. Completing the STIRAP cycle then maps the system to an atomic state that depends on the position of the atom in the dressed state Rabi-cycle. Results that we have obtained for this procedure are shown in Fig. 3a. The Rabi oscillations are sustained over 550 ms demonstrating the long-lived coherence of the dressed states when driven by rf radiation.

These experiments also demonstrate that coherent transfer to the dressed state basis and subsequent application of a Rabi pulse prepares a coherent superposition in the qubit space that can then be read out efficiently after completion of the STIRAP cycle. This in turn forms the basis for the measurements of the lifetime of coherent superpositions in the protected subspace that we are now turning to.

These Ramsey-type experiments test the dephasing time of the dressed state qubit. Fig. 3b shows that coherence is preserved for more than 1000 ms, close to the ultimate limit of about 1700 ms set by the lifetime of the state  $|D\rangle$  and more than two orders of magnitude longer than the dephasing time of the atomic states  $|-1\rangle$  and  $|+1\rangle$  making this scheme ideal for realizing a quantum memory.

*Coupling qubit to motion* — The realization of multi-qubit gates can be achieved by coupling the electronic qubit to the motion of the ions [10, 11, 25]. Several schemes for realizing such conditional quantum dynamics are possible using dressed states. Here we outline the scheme illustrated in Fig. 1b.

This can be achieved by using a pair of rf-fields on the  $|0'\rangle \leftrightarrow | \pm 1\rangle$  transitions. These rf fields are detuned by the vibrational mode frequency  $\nu$  from this carrier and are thus in resonance with the first motional side band (compare Fig. 1b). In the dressed state basis, this couples the  $|D\rangle \leftrightarrow |0'\rangle$  qubit resonance of the protected subspace to the vibrational mode of the ion string. The coupling  $|B\rangle \leftrightarrow |0'\rangle$  in zeroth order in the Lamb-Dicke parameter (carrier transition) will be canceled in the rotating wave approximation (RWA) due to the higher energy (by  $\Omega$ ) of the  $|B\rangle$  state, and state  $|D\rangle$  will be coupled only in first order in the Lamb Dicke parameter such that we obtain a Hamiltonian of the form (see Methods for details)

$$H = \sqrt{2}\eta\Omega_g (|D\rangle \langle 0'| e^{i\delta t} + h.c) (b^+ - b). \quad (1)$$

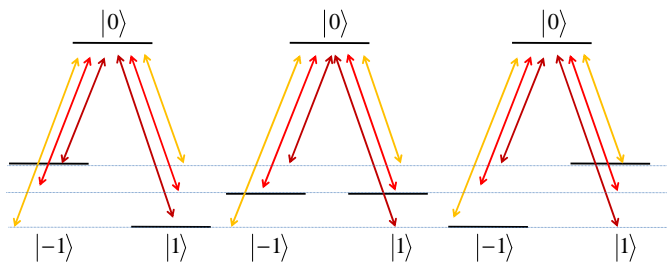


FIG. 4. Multi-qubit scheme. Energy level representation of three ions along a gradient of magnetic field. The magnetic field on the two external ions has the same magnitude but opposite direction producing opposite symmetrical Zeeman energy shifts on the levels  $|-1\rangle$  and  $|1\rangle$ . The arrows represent three pairs of microwave frequencies from a comb with frequency interval corresponding to the Zeeman shift between two ions. Each frequency pair (identified by its own color) is only resonant with one ion.

Importantly, since this gate has no carrier part, a small Lamb-Dicke parameter  $\eta$  can be compensated for by increasing the rf power while obeying  $\eta\Omega_g \ll \nu$ . This will allow for working with moderate static [5, 6, 12] or oscillating [7] magnetic field gradients when utilizing rf or microwave radiation for multi-qubit quantum gates. Also, this scheme permits the realization of other types of gates including gates with ions in thermal motion [10, 11].

*Multi-qubit quantum processor* — To complete the elements of a universal QIP device based on microwave dressed states we will now outline how the dressed state scheme for QIP can be applied to a collection of trapped ions. The long wavelength of the microwave radiation requires the use of a static magnetic field gradient, if individual addressing in frequency space is desired. A gradient of a static or oscillating magnetic field is required for the generation of the coupling of the electronic degrees of freedom to the motional degrees of freedom when microwave or rf radiation is used for quantum gates. Therefore, this does not represent an additional experimental requirement.

In the absence of a static magnetic field gradient, a single pair of microwave dressing fields is sufficient to dress all ions. In the presence of static gradient each ion would require its own pair of driving fields. This can be accomplished efficiently by employing a microwave frequency comb where the frequency spacing coincides with the change in Zeemann shift between neighbouring ions as shown in Fig. 4. Then, for each ion two microwave fields in the comb are resonant with the relevant atomic transition, dressing and shifting the states  $|u\rangle$  and  $|d\rangle$ . For each off-resonant microwave field with detuning  $\Delta$  there is a second field with equal and opposite detuning  $-\Delta$ . Hence each such off-resonant pair will only couple to  $|B\rangle$  leading to equal and opposite Stark-shifts which then cancel. Thus the dressed state structure for each ion remains essentially the same as in the single ion case achieving a robust memory. Small errors due to higher order effects may be introduced and the execution of gates on ions may lead to off-resonant transitions and hence phase shifts in other ions. However, it is important to note that the amount of this error is exactly as for MAGIC [6]. This is due to the fact that the microwave fields almost completely decouple the  $\{|u\rangle, |d\rangle\}$  subspace from the qubit subspace  $\{|D\rangle, |0'\rangle\}$  as long as  $\Omega$  (the dressing field Rabi frequency) is much larger (typically, an order of magnitude) than the rf coupling  $\Omega_g$ . The reason for this decoupling is the large energy gap between the qubit subspace and the  $\{|u\rangle, |d\rangle\}$  subspace. For both single qubit gates and multi-qubit gates, individual addressing is achieved by choosing the frequency of the rf field. Corrections are small under the condition  $\Omega_g \ll \Delta E_Z/\hbar$  where  $\Delta E_Z$  is the difference in Zeeman shifts between two neighbouring ions. An important advantage over the regular quantum computing scheme is that the carrier and the sideband can be chosen by interference and not by setting the frequency on resonance with one of these transitions; i.e., the choice is set by the phase difference between the two rf drives. This enables fast gates which are not limited to  $\Omega_g \ll \nu$  but by  $\eta\Omega_g \ll \nu$ .

In conclusion, we have shown that by using a dressed four level system, qubits can be realized that are resilient to magnetic field noise which otherwise imposes a barrier for the coherence time in various implementations of QIP. Still, the dressed states' ability to support microwave-based conditional quantum dynamics is preserved. Detailed experimental investigations of the preparation and detection of microwave-dressed states have been conducted, and measurements of the lifetime of dressed states and of the coherence time of superpositions of dressed qubit states are reported revealing an improvement compared to atomic states by more than two orders of magnitude. It is shown that dressed states allow for fast multi-qubit gates even in the presence of a small effective Lamb-Dicke parameter, and that scaling to arrays of trapped ions is possible. The insight gained in this work removes a major obstacle for laser-free quantum information processing (but is also applicable to laser-based schemes). Furthermore, this scheme is not restricted to trapped ions and is in fact applicable to other physical systems where dephasing due to external

perturbations plays a role, for instance, neutral atoms [26] and solid state systems such as NV-centres in diamond [27], ion-doped crystals [27], and circuit-QED [28].

## METHODS

### The experimental system

Transitions between ground state hyperfine levels of a single  $^{171}\text{Yb}^+$  ion confined in a miniature Paul trap (diameter of 2 mm) are driven with microwave radiation close to 12.64 GHz [29] which is generated by mixing the signal from a fixed frequency source at 6.3 GHz with an rf signal whose frequency, amplitude, and phase are adjustable. For STIRAP, two microwave fields are used with Gaussian amplitude envelopes shifted in time relative to each other driving the  $|-1\rangle \leftrightarrow |0\rangle$  and the  $|+1\rangle \leftrightarrow |0\rangle$  transitions, respectively (see Fig. 1)

$^{171}\text{Yb}^+$  is produced from its neutral precursor by photoionization using a diode laser operating near 399 nm. Laser light near 369 nm driving resonantly the  $S_{1/2} F = 1 \leftrightarrow P_{1/2} F = 0$  transition in  $\text{Yb}^+$  is supplied by a frequency doubled Ti:Sa laser, and serves for cooling and state selectively detecting the ion. Initialization in the state  $S_{1/2} F = 0$  ( $|0\rangle$ ) is done using 369 nm light tuned to the  $S_{1/2} F = 1 \rightarrow P_{1/2} F = 1$  transition. A diode laser delivers light near 935 nm and drives the  $D_{3/2} \leftrightarrow [3/2]_{1/2}$  transition to avoid optical pumping into the metastable  $D_{3/2}$  state during the cooling and detection periods.

The effectiveness of the STIRAP process for creating dressed states and transferring them into the final state has been investigated as a function of the parameters characterizing the pulse sequence (compare [30] for optical STIRAP). The sequence is divided into discrete time increments  $\Delta t = 1/(f_\Omega N_t)$  with a positive integer  $N_t$  and  $f_\Omega = \Omega/(2\pi)$  where  $\Omega$  is the peak Rabi frequency. The width of the Gaussian pulses is given by  $N/f_\Omega$ , with an integer number  $N$ . The STIRAP sequence is robust against variations of these parameters: we investigated the range  $10 \leq N_t \leq 40$  for fixed  $N = 10$  and found no variation in the effectiveness of the pulse sequence, that is, the overall fidelity of initial preparation of  $|0\rangle$ , preparation of  $|D\rangle$ , and read-out stays constant (within statistical variations) at a value of about 93%

When measuring sequences with pulse widths varying in the range  $2 \leq N \leq 20$  equally good results were obtained for  $N \geq 4$ . The separation in time  $s_t/f_\Omega$  of the two Gaussian pulses was varied over the range  $0 \leq s_t/f_\Omega \leq 40/f_\Omega$ , for a pulse width where  $N = 10$  to obtain a plateau of high effectiveness ( $\approx 93\%$ ) for the number  $s_t$  belonging to the interval  $10 \leq s_t \leq 20$ . The best performance is obtained for equal detunings  $\Delta_+ = \Delta_-$ , ideally  $\Delta_+ = 0 = \Delta_-$ , and for small relative detunings. An experimental investigation yielded for  $|\delta| = |\Delta_+ - \Delta_-| < 0.1\Omega$  no statistically significant variation of the dressed state preparation fidelity.

In order to prepare, for example, the  $|D\rangle$  state, the population is first transferred from the initial state  $|0\rangle$  to the atomic state  $|-1\rangle$  by applying a microwave  $\pi$ -pulse. The first half of the STIRAP sequence then transfers the atomic population to the dressed state  $|D\rangle$ .

A hold in the evolution of the two STIRAP microwave fields is introduced at the crossing point of the amplitude envelopes of the two pulses. At this point in time the occupation of the  $|D\rangle$  state is at its maximum. Any dephasing of the  $|D\rangle$  state or transitions to other states during the holding time  $T$  gives rise to imperfect population transfer during the second half of the STIRAP sequence that transfers the system to the atomic state  $|+1\rangle$ .

Probing the state after the complete STIRAP sequence does not distinguish between  $|-1\rangle$  and  $|+1\rangle$ , as both yield bright results upon final detection of resonance fluorescence. Therefore, a  $\pi$ -pulse swaps the population of  $|+1\rangle$  and  $|0\rangle$  before final detection. Thus, a dark result indicates a successful STIRAP transfer between atomic states and dressed states and a lifetime  $T$  of the dressed state prepared during the the holding period. The effectiveness of the STIRAP sequence as a function of the holding time  $T$  is shown in Fig. 2.

In order to record Rabi oscillations between dressed states we first prepare state  $|B\rangle$ , then an rf pulse in resonance with  $|0'\rangle \leftrightarrow |\pm 1\rangle$  (Fig. 1a) is applied during the hold time  $T$  in the evolution of STIRAP. This rf-pulse induces Rabi oscillations between  $|B\rangle$  and  $|0'\rangle$ . After the Rabi pulse, the STIRAP pulse sequence is completed and the population of the atomic state  $|0\rangle$  is probed as described above. If during the rf Rabi pulse state  $|0'\rangle$  is populated, then the second part of the STIRAP sequence has no effect, that is,  $|0\rangle$  is not populated at the end of the experimental sequence.

### Theory: Single-qubit gate

Starting with the Hamiltonian

$$H_{sqg} = \omega_0 |0\rangle \langle 0| + \lambda_0 (|1\rangle \langle 1| - |-1\rangle \langle -1|) +$$

$$\begin{aligned} & \Omega (|-1\rangle \langle 0| e^{-i\omega_{-1}t} + |1\rangle \langle 0| e^{-i\omega_1 t} + h.c) + \\ & \Omega_g (|-1\rangle \langle 0'| e^{-i\lambda_0 t} - |1\rangle \langle 0'| e^{i\lambda_0 t} + h.c) \end{aligned} \quad (2)$$

if we set  $\omega_{-1} = \omega_0 + \lambda_0$ ,  $\omega_1 = \omega_0 - \lambda_0$ , moving to the interaction picture with respect to the time independent part we get:

$$\begin{aligned} H_{sqg}^I &= \sqrt{2}\Omega (|B\rangle \langle 0| + h.c) + \sqrt{2}\Omega_g (|D\rangle \langle 0'| + h.c) \\ &= \frac{\Omega}{\sqrt{2}} |u\rangle \langle u| - \frac{\Omega}{\sqrt{2}} |d\rangle \langle d| + \sqrt{2}\Omega_g (|D\rangle \langle 0'| + h.c) \end{aligned} \quad (3)$$

The first two terms shift states  $|u\rangle$  and  $|d\rangle$  (that both contain  $|B\rangle$ ) away from the  $|D\rangle$ , and the second part creates the gate. The interactions created by the two microwave fields with Rabi frequency  $\Omega$  and the rf field  $\Omega_g$  shown in Fig. 1a permit the implementation of this Single-qubit gate. The two rf fields have a  $\pi$  phase difference at the initial time of the pulse which realizes the coupling to the  $|D\rangle$  state and not the  $|B\rangle$  state.

### Theory: Multi-qubit gate

The levels and fields of Fig. 1b are described by the Hamiltonian:

$$\begin{aligned} H_{mqg}^I &= \omega_0 |0\rangle \langle 0| + \lambda_0 (|1\rangle \langle 1| - |-1\rangle \langle -1|) + \\ & \Omega (|-1\rangle \langle 0| e^{-i\omega_{-1}t} + |1\rangle \langle 0| e^{-i\omega_1 t} + h.c) + \\ & \Omega_g (|-1\rangle \langle 0'| e^{-i(\lambda_0 - \delta)t} + |1\rangle \langle 0'| e^{i(\lambda_0 - \delta)t} + h.c) \\ & + \nu b^+ b_1 |1\rangle \langle 1| + \lambda (|-1\rangle \langle -1| - |1\rangle \langle 1|) (b + b^+), \end{aligned} \quad (4)$$

where  $b$  and  $b^+$  are the annihilation and creation operators of the trap and  $\lambda$  is proportional to the magnetic gradient as in [6]. In the interaction picture with respect to the microwaves and after the Polaron transformation:

$U = e^{\eta|+1\rangle\langle +1|(b^+ - b)} e^{-\eta|-1\rangle\langle -1|(b^+ - b)}$  we get:

$U H U^\dagger = \nu b^+ b + \Omega_g (|-1\rangle \langle 0'| e^{-\eta(b^+ - b)} e^{i\delta t} + |1\rangle \langle 0'| e^{\eta(b^+ - b)} e^{i\delta t} + h.c)$ . In first order in the Lamb Dicke parameter we get:

$$\sqrt{2}\eta\Omega_g (|D\rangle \langle 0'| e^{i\delta t} - h.c) (b^+ - b) \quad (5)$$

In zeroth order we get a coupling between the  $|B\rangle$  and  $|0'\rangle$ , this term is ignored since the coupling  $\Omega_g$  is much smaller than the energy gap which is of the order  $\Omega$ . Note however, that by changing the phase between the rf fields a gate with respect to the  $|B\rangle$  state can be realized.

- 
- [1] Blatt, R. & Wineland, D. Entangled states of trapped atomic ions. *Nature* **453**, 1008-1015 (2008) and references therein.
  - [2] Friedenauer, A. Schmitz, H. Glueckert, J. T. Porras, D. & Schaetz, T. Simulating a quantum magnet with trapped ions. *Nat Phys* **4**, 757-761 (2008).
  - [3] Kim, K. *et al.* Quantum simulation of frustrated Ising spins with trapped ions. *Nature* **465**, 590-593 (2010).
  - [4] Gerritsma, R. *et al.* Quantum simulation of the Dirac equation. *Nature* **463**, 68-71 (2010).
  - [5] Johanning, M. Varón, A. F. & Wunderlich, C. Quantum simulations with cold trapped ions. *J. Phys. B* **42**, 154009 (2009) and references therein.
  - [6] Mintert, F. & Wunderlich, C. Ion-Trap Quantum Logic Using Long-Wavelength Radiation. *Phys. Rev. Lett.* **87**, 257904 (2001).
  - [7] Ospelkaus, C. *et al.* Trapped-Ion Quantum Logic Gates Based on Oscillating Magnetic Fields. *Phys. Rev. Lett.* **101**, 090502 (2008).
  - [8] Ozeri, R. *et al.* Errors in trapped-ion quantum gates due to spontaneous photon scattering. *Phys. Rev. A* **75**, 042329 (2007).
  - [9] Plenio, M. B. & Knight, P. L. Decoherence limits to quantum computation using trapped ions. *Proc. R. Soc. Lond. A* **453**, 2017-2041 (1997).
  - [10] Sørensen, A. & Mølmer, K. Entanglement and quantum computation with ions in thermal motion. *Phys. Rev. A* **62**, 022311 (2000).

- [11] Milburn, G. J. Schneider, S. & James, D. F. V. Ion trap quantum computing with warm ions. *Fortschr. Phys.* **48**, 801-810 (2000).
- [12] Wunderlich, C. in *Laser Physics at the Limit* (eds Meschede, D. Zimmermann, C. & Figger, H.) (Springer, 2002).
- [13] Wunderlich, C. & Balzer, C. Quantum measurements and new concepts for experiments with trapped ions. *Adv. At. Mol. Phys.* **49**, 293-372 (2003).
- [14] Mc Hugh, D. & Twamley, J. Quantum computer using a trapped-ion spin molecule and microwave radiation. *Phys. Rev. A* **71**, 012315 (2005).
- [15] Wang, S. X. Labaziewicz, J. Ge, Y. Shewmon, R. & Chuang, I. L. Individual addressing of ions using magnetic field gradients in a surface-electrode ion trap. *Appl. Phys. Lett.* **94**, 094103 (2009).
- [16] Johanning, M. *et al.* Individual Addressing of Trapped Ions and Coupling of Motional and Spin States Using rf Radiation. *Phys. Rev. Lett.* **102**, 073004 (2009).
- [17] Häffner, H. *et al.* Robust entanglement. *Appl. Phys. B* **81**, 151-153 (2005).
- [18] Kielpinski, D. *et al.* A Decoherence-Free Quantum Memory Using Trapped Ions. *Science* **291**, 1013-1015 (2001).
- [19] Home, J. P. *et al.* Complete Methods Set for Scalable Ion Trap Quantum Information Processing. *Science* **325**, 1227-1230 (2009).
- [20] Viola, L. & Lloyd, S. Dynamical suppression of decoherence in two-state quantum systems. *Phys. Rev. A* **58**, 2733 (1998).
- [21] Rabl, P. *et al.* Strong magnetic coupling between an electronic spin qubit and a mechanical resonator. *Physical Review B* **79**, 041302 (2009).
- [22] Biercuk, M. J. *et al.* Optimized dynamical decoupling in a model quantum memory. *Nature* **458**, 996-1000 (2009).
- [23] Bluhm, H. *et al.* Dephasing time of GaAs electron-spin qubits coupled to a nuclear bath exceeding 200 $\mu$ s. *Nature Phys.* **7**, 109-113 (2011).
- [24] Vitinov, N. V. Fleischhauer, M. Shore, B. W. & Bergmann, K. Coherent manipulation of atoms and molecules by sequential laser pulses. *Adv. At. Mol. Phys.* **46**, 55-190 (2001).
- [25] Cirac, J. I. & Zoller, P. Quantum Computations with Cold Trapped Ions. *Phys. Rev. Lett.* **74**, 4091 (1995).
- [26] Specht, H. P. *et al.*, A Single-Atom Quantum Memory, arXiv:1103.1528 (2011).
- [27] Simon, C. *et al.* Quantum memories. *Eur. Phys. J. D* **58**, 1-22 (2010).
- [28] Clarke, J. & Wilhelm, F. K. Superconducting quantum bits. *Nature* **453**, 1031-1042 (2008).
- [29] Hannemann, T. *et al.*, Self-learning estimation of quantum states. *Phys. Rev. A* **65**, 050303 (2002).
- [30] Sørensen, J. *et al.* Efficient coherent internal state transfer in trapped ions using stimulated Raman adiabatic passage. *New J. Phys.* **8**, 261 (2006).

## ACKNOWLEDGMENTS

We acknowledge support by the Bundesministerium für Bildung und Forschung (FK 01BQ1012), Deutsche Forschungsgemeinschaft, European Commission under the STREPs PICC and GIF, secunet AG, and the Alexander von Humboldt Foundation. Technical help with the microwave set-up by T. F. Gloger is acknowledged.